ORIGINAL ARTICLE

Statistical Optimization of Green Synthesized Silver Nanoparticles Using *Syzygium cumini* Leaf Extract through Central Composite Design and Antidiabetic Applications

Veeranna S. Hombalimath[1], Uday M. Muddapur[1], Shrawani Ganesh Dasa[1], Salah Eldeen Dafallah[2,3], Laxmikant R. Patil[1], Anil R. Shet[1], AbdulAzeem A. Khan[4], Ibrahim Ahmed Shaikh[5], Gurumurthy Mahadevan Dummi[6], Aejaz Abdullatif Khan[7], Syed Mohammed Shakeel Iqubal[7], Tasneem Mohammed[7]

[1]Department of Biotechnology, KLE Technological University, Hubballi, Karnataka, India, [2]Department of Anatomy, Ibn Sina National College for Medical Studies, Jeddah, Saudi Arabia, [3]University of Eastern Sudan for Medical Sciences and Technology, Port Sudan, Sudan, [4]Department of CSE (AIML), KLS Gogte Institute of Technology (Autonomous) Affiliated to Visvesvaraya Technological University, Belagavi, Karnataka, India, [5]Department of Pharmacology, College of Pharmacy, Najran University, Najran, Saudi Arabia, [6]Molecular Genetic Laboratory, Amity Institute of Biotechnology, Amity University, Noida, Uttar Pradesh, India, [7]Department of General Science, Ibn Sina National College for Medical Studies, Jeddah, Saudi Arabia

Abstract

Aims: This study reports the eco-friendly synthesis of silver nanoparticles (AgNPs) using *Syzygium cumini* leaf extract under a range of pH conditions (3–9), with optimal nanoparticle formation observed at pH 9 as evidenced by ultraviolet-visible spectroscopy. **Materials and Methods:** Comprehensive characterization techniques, including X-ray diffraction (XRD), scanning electron microscopy (SEM), and Fourier-transform infrared spectroscopy (FTIR), were employed to elucidate the properties of the synthesized AgNPs. **Results and Discussion:** XRD analysis confirmed the crystalline nature of the nanoparticles, revealing an average size of 21.63 nm, while SEM imaging demonstrated predominantly spherical morphologies with occasional aggregation. FTIR studies identified key functional groups from the leaf extract involved in nanoparticle stabilization. The synthesis process was further optimized using response surface methodology with a central composite design, which identified silver nitrate concentration as a critical parameter. Notably, the synthesized AgNPs exhibited significant concentration-dependent anti-diabetic activity, achieving approximately 43% enzyme inhibition at 150 µg/mL, likely due to interactions with α-amylase or α-glycosidase that modulate glucose metabolism. **Conclusion:** These results underscore the promising biomedical potential of green-synthesized AgNPs, particularly for diabetes management, and highlight the advancement of sustainable nanotechnology approaches.

Key words: Anti-diabetic, antimicrobial, characterization, green synthesis, optimization, phytochemicals, silver nanoparticles, *Syzygium cumini*

INTRODUCTION

Throughout India's verdant landscapes, medicinal plants and their derivatives are widely accessible and reasonably priced. For centuries, these herbs have been widely used in Ayurvedic medicine.[1] In recent years, many of these plants have gained recognition due to their unique bioactive

Address for correspondence:
Veeranna S. Hombalimath, Department of Biotechnology, KLE Technological University, Hubballi, Karnataka, India. E-mail: hombalimath@kletech.ac.in

Received: 21-07-2025
Revised: 12-09-2025
Accepted: 20-09-2025

compounds and diverse applications in emerging research and development fields.[2] *Syzygium cumini*, commonly known as "Jamun" in Hindi or "blackberry of India," belongs to the Myrtaceae family and thrives in tropical regions, particularly in humid America and Australia. Although it predominantly grows in moist and sub-moist climatic conditions worldwide. This plant has been widely used in traditional medicine for treating various ailments.[3] Every part of *S. cumini* possesses medicinal properties and has been used since ancient times to treat conditions such as asthma, bronchitis, sore throats, biliousness, diarrhea, and excessive thirst. The bark of the tree acts as a blood purifier, traditionally used for its therapeutic benefits. The fruit was known for its astringent, acrid, sweet, and cooling properties, helping to eliminate foul mouth odor while also exhibiting stomachic, astringent.[4] The fruit and leaves, with a longstanding history of medicinal application, are currently utilized to address chronic diarrhea and other gastrointestinal disorders. In addition, the seeds are known for their astringent, and are particularly beneficial in managing diabetes. The ash derived from the leaves also holds medicinal significance. The ash derived from the leaves of *S. cumini* has been traditionally used to strengthen teeth and gums. Vinegar made from the juice of its ripe fruit serves as an effective stomachic and carminative, exhibiting diuretic properties while also being beneficial for spleen enlargement and acting as an astringent in chronic diarrhea. Due to its considerable medicinal properties, the plant was chosen for the current study.[5]

Green synthesis has emerged as a superior alternative to traditional chemical and physical methods due to its cost-effectiveness, environmental sustainability, and scalability for large-scale production. Unlike traditional methods, it eliminates the need for high pressure, excessive energy consumption, elevated temperatures, or hazardous chemicals. Plant-based nanoparticle synthesis offers a more efficient approach compared to other biological methods, this approach circumvents the intricate and time-intensive procedures associated with cell culture maintenance, facilitating large-scale production in non-sterile settings.[6] The synthesis of nanoparticles through plant extracts is both cost-effective and offers a sustainable alternative for the large-scale production of metal nanoparticles. Plant extracts serve dual roles as reducing and stabilizing agents. Silver nanoparticles (AgNPs) are a subject of extensive research regarding their synthesis, stabilization, and diverse applications.[7] Nanoscience and nanotechnology are at the forefront of research in combating infections caused by multidrug-resistant strains. Nanomedicine has demonstrated remarkable potential in addressing microbial infections, with nanoparticle-based technologies playing a crucial role. Plant-mediated synthesis of nanoparticles was gaining popularity due to its simplicity, rapid blend process, and eco-friendliness. AgNPs are among the most widely studied and synthesized nanomaterial.[8] The synthesis of AgNPs was first validated through surface Plasmon resonance through ultraviolet-visible (UV-Vis) spectroscopy, subsequently analyzed using transmission electron microscopy (TEM), which demonstrated their spherical morphology. AgNPs exhibit significant antibacterial, anti-inflammatory, antiviral, anti-angiogenesis, and anti-platelet properties, which underscores their importance in medical applications. Utilizing plant leaf extracts for the synthesis of nanoparticles notably decreases expenses and removes the necessity for intricate microbial culture setups and sterile environments.[9]

Plants contain a variety of biomolecules, including carbohydrates, proteins, and coenzymes, which help in the reduction of metallic salts to nanoparticles. Compared to chemical synthesis, the photosynthesis of nanoparticles was a more environmentally sustainable approach, as plant extracts contain active biomolecules like polyphenols that facilitate the reduction of silver ions to AgNPs. AgNPs are valued for its exceptional antimicrobial properties, and while various methods including chemical, photochemical, biological, radiation, laser, and electrochemical methods are employed to create AgNPs.[10] AgNPs exhibit unique physicochemical and biological properties beyond bulk silver. They have the capability to bind to bacterial cell walls, penetrate the membrane, induce structural damage causing cellular contents to leak, which eventually results in bacterial death. Cell wall thickness variations are the cause of this variation. The peptidoglycan layer of gram-positive bacteria is thicker (30 nm), while Gram-negative bacteria have a thinner (3–4 nm) layer. In addition, carboxyl, phosphate, and amino groups are examples of negatively charged functional groups found in bacterial cell membranes. Which interact electrostatically with positively charged AgNPs, facilitating their adhesion and penetration into bacterial cells.[11]

Small-volume AgNPs, with their higher surface-area-to-volume ratio, exhibit stronger antibacterial effects by more frequently interacting with bacterial cells. Once inside the microbial cell, AgNPs interact with cellular organizations and biomolecules, including proteins, lipids, and DNA, disrupting essential cellular functions and leading to cell death. Particularly, AgNPs interfere with ribosomal activity, causing protein synthesis inhibition, leading to cellular dysfunction.[12] This study examines the stability and versatility of AgNPs in biomedical applications, emphasizing the green synthesis of cost-effective and eco-friendly bioactive AgNPs derived from fruit extracts of *S. cumini*. The synthesized nanoparticles underwent characterization and assessment for their *in vitro* antioxidants, antibacterial, and anti-inflammatory properties. These findings will serve as preliminary data for future studies.[13]

This study focused on creating an environmentally friendly and sustainable approach for the synthesis of AgNPs utilising *S. cumini* leaf extract, optimize the synthesis conditions, characterize the resulting nanoparticles, and evaluate their potential biomedical applications, particularly their anti-diabetic activity. This method uses the inherent reducing

and stabilizing agents found in the plant extract to facilitate effective nanoparticle formation. While also exploring the therapeutic potential of the synthesized AgNPs in modulating glucose metabolism for diabetes management.

MATERIALS AND METHODS

S. cumini, commonly known as jamun, was a remarkable tropical evergreen tree from the Myrtaceae family that was taken from Hubballi, Karnataka state for studies.[14] Beyond its lush foliage and deep purple fruits, *S. cumini* holds significant ecological and economic value [Figure 1a]. It serves an essential function in the production of fruit, timber supply, and ornamental landscaping. Ecologically, it supports biodiversity, prevents soil erosion, and contributes to carbon sequestration. Economically, its nutrient-rich fruits are widely consumed, its durable wood was used in construction, and its medicinal properties make it valuable in pharmaceuticals. In addition, its resilience to drought and pollution makes it ideal for urban greenery and reforestation projects.

Preparation of plant extract

Silver nitrate was chosen as the precursor for nanoparticle synthesis. AgNPs were prepared by reacting *S. cumini* leaf extract with a 10 mM aqueous solution of $AgNO_3$ (Merck) [Figure 1b]. Equal volumes (1:1, v/v) of silver nitrate solution and leaf extract were mixed in a 100 mL flask, which was wrapped in aluminum foil to prevent photoactivity. The flasks underwent incubation for a duration of 1-8 h at varying pH levels (3, 5, 7, and 9) to optimize biogenic nanoparticle synthesis. Preliminary confirmation of the synthesis of nanoparticle was confirmed using a UV-Vis spectrophotometer. Then solution was centrifuged at 14,000 rpm for 10 min, and resulting pellets were washed 3 times with distilled water to remove other contaminants. The pellet was subsequently placed onto a petri plate and subjected to drying in an oven at a temperature range of 60–70°C. After drying, the nanoparticles were carefully scraped off, ground into a fine black powder with a mortar and pestle and subsequently stored in Falcon tubes at room temperature for further characterization and bioactivity studies.[15,16]

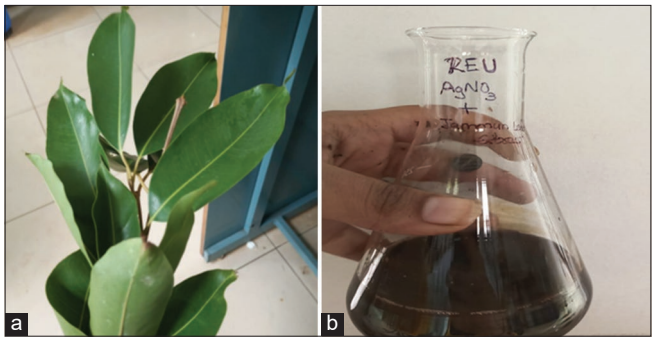

Figure 1: (a) *Syzygium cumini*, plant leaves. (b) Plant extract

Mass production of AgNPs

The aqueous extract was amalgamated with a 1mM $AgNO_3$ solution in a 1:9 ratio, wherein 900 mL of the 1mM $AgNO_3$ solution was prepared and combined with 100 mL of the aqueous extract. The resulting colloidal solution was incubated for 24 h in a flask wrapped with silver foil and stored in the dark place. The observed color transformation from colorless to reddish-brown indicated the reduction of Ag+ to its oxide. Following incubation, the produced nanoparticles were separated from the mixture by centrifuging it for 20 min at 6000 rpm. After being gathered, the pellets were put into petri dishes and allowed to dry in a hot air oven. After being carefully scraped from the petri dishes, the dried AgNPs were placed in Eppendorf tubes for further analysis and characterization. This methodical process ensures the production and collection of AgNPs for further scientific investigation and potential applications.[16,17]

Response surface methodology (RSM)

Response surface methodology in conjunction with face-centered central composite design was used to optimize the experimental conditions, including pH, extract volume, and $AgNO_3$ volume. In Minitab 17, Tables 1 and 2 summarized the variable ranges and results from 20 experiments.

The analysis of variance table evaluates the influence of pH, extract volume, and $AgNO_3$ volume on the response variable associated with AgNP synthesis. The model demonstrated statistical significance (P = 0.019), suggesting that at least one factor has a notable impact on the response. Among the linear terms, $AgNO_3$ volume (P = 0.002) exhibited a highly significant effect, whereas pH (P = 0.080) and extract volume (P = 0.556) did not. A significant quadratic effect was observed for (extract volume)^2 (P = 0.032), indicating a nonlinear relationship, while pH^2 (P = 0.183) and ($AgNO_3$ volume)^2 (P = 0.861) were not significant. Interaction effects were also non-significant (P > 0.05), suggesting that the combined influence of these factors does not affect the response. The lack-of-fit test (P = 0.206) was not significant, confirming that the model appropriately fits the data. Overall, the findings indicate that $AgNO_3$ volume plays a crucial role in AgNPs synthesis, with a potential nonlinear effect from extract volume.[18]

The contour plot [Figure 2a] illustrates the variation in the wavelength of Jamun extract as a function of pH and the volume

Table 1: The levels and ranges of the independent variables

Parameters	−α	−1	0	1	α
pH	5.97	7	8.5	10	11.02
Volume of extract	0.81	1.5	2.5	3.5	4.18
Volume of $AgNO_3$	16.6	20	25	30	33.41

Table 2: Design of experiments, central composite design for synthesis of silver nanoparticles and analysis of variance

Source	DF	Adj SS	Adj MS	F-value	*P*-value
Model	9	4036.72	448.52	4.13	0.019
Linear	3	2268.09	756.03	6.97	0.008
pH	1	410.38	410.38	3.78	0.080
Volume of extract	1	40.28	40.28	0.37	0.556
Volume of $AgNO_3$	1	1817.42	1817.42	16.75	0.002
Square	3	987.26	329.09	3.03	0.080
pH^2	1	222.24	222.24	2.05	0.183
$(\text{Volume of extract})^2$	1	677.47	677.47	6.24	0.032
$(\text{Volume of } AgNO_3)^2$	1	3.49	3.49	0.03	0.861
2-Way interaction	3	781.37	260.46	2.40	0.129
pH×volume of extract	1	351.12	351.12	3.24	0.102
pH×volume of $AgNO_3$	1	325.12	325.12	3.00	0.114
(Volume of extract)×(Volume of $AgNO_3$)	1	105.13	105.13	0.97	0.348
Error	10	1085.28	108.53		
Lack-of-Fit	5	743.94	148.79	2.18	0.206
Pure error	5	341.33	68.27		
Total	19	5122.00			

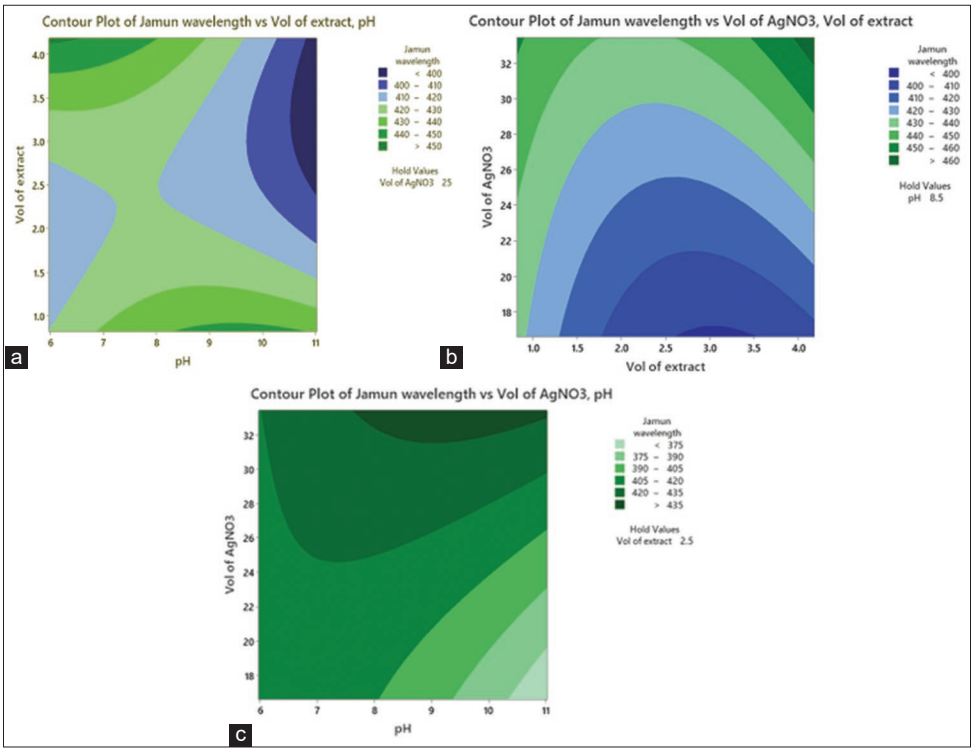

Figure 2: (a) Contour plot of volume of extract versus pH. (b) Contour plot volume of $AgNO_3$ versus volume of extract. (c) Contour plot volume of $AgNO_3$ versus pH

of extract while maintaining a fixed $AgNO_3$ concentration of 25. Different color regions represent distinct wavelength ranges, with darker shades indicating lower wavelengths (<400 nm) and lighter shades representing higher values (>450 nm). The plot suggests that wavelength shifts are influenced by both pH and extract volume, with noticeable changes occurring at higher pH levels and lower extract volumes. Such variations can be attributed to alterations in the optical properties of the extract, likely due to pH-dependent molecular interactions or nanoparticle formation. This

contour analysis provides insight into the tunability of Jamun-based nanoparticle synthesis and its potential applications in nanomaterial's research.[19]

The contour plot [Figure 2b] shows how variations in pH and extract volume affect the wavelength of AgNPs made with jamun extract, while maintaining a constant $AgNO_3$ concentration of 25 mM. Darker regions on the plot correspond to lower wavelengths (<400 nm), indicating smaller nanoparticle sizes, whereas lighter regions represent higher wavelengths (>450 nm), suggesting larger nanoparticles. The plot reveals that at higher pH levels and lower extract volumes, there is a significant shift toward shorter wavelengths, implying the formation of smaller AgNPs. This trend is consistent with findings from other studies; for instance, research using *Alpinia katsumadai* seed extract demonstrated that increasing the smaller nanoparticles with absorption peaks shifting from 417 nm to 436 nm are formed when pH speeds up the reduction of Ag^+ ions. Similarly, a study involving *Citrullus lanatus* fruit rind extract observed a blue shift in UV-Vis absorption peaks as pH increased from 8 to 10, indicating a reduction in nanoparticle size.[20]

The contour plot [Figure 2c] shows how different pH levels and extract volumes relate to the wavelength of AgNPs made with jamun extract, while maintaining a constant $AgNO_3$ concentration of 25 mM. Darker regions on the plot correspond to lower wavelengths (<400 nm), indicating the formation of smaller nanoparticles, whereas lighter regions represent higher wavelengths (>450 nm), suggesting larger nanoparticles. The plot reveals that at higher pH levels and lower extract volumes, there is a significant shift toward shorter wavelengths, implying the formation of smaller AgNPs. This trend is consistent with findings from other studies; for instance, research using *A. katsumadai* seed extract demonstrated that increasing the pH accelerates the reduction of Ag^+ ions, leading to the formation of smaller nanoparticles with absorption peaks shifting from 417 nm to 436 nm. Similarly, a study involving *Pometia pinnata* (Matoa) leaf extract found that at higher pH levels, the synthesis of AgNPs was more efficient, resulting in nanoparticles with varied shapes and sizes, as confirmed by UV-Vis spectroscopy and TEM. In addition, research utilizing *C. lanatus* (watermelon) rind extract observed that increasing the pH from 6 to 10 led to a blue shift in the UV-Vis absorption peaks, indicating a reduction in nanoparticle size.[21,22]

Characterization of AgNPs

Various analytical techniques, including UV-Vis spectrophotometry, Fourier-transform infrared spectroscopy (FTIR), X-ray diffraction (XRD), and scanning electron microscopy (SEM), were used to characterize the biosynthesized AgNPs, assessing their quality, structure, and composition.[23] UV-Vis spectrophotometry (200–800 nm) confirmed AgNP formation through a characteristic color change from deep brown to blackish, indicating Ag^+ ion reduction [Figure 3]. UV-Vis analysis at varying pH levels showed no peak was shown at pH 3, while pH 5, 7, and 9 exhibited increasing absorbance; maximum peak was absorbed at pH 9.

FTIR spectroscopy (Shimadzu Model 270) identified biomolecules interacting with AgNPs, using a KBr-AgNPs mix (1:100) with absorbance recorded from 400 to 4000 cm^{-1}. The reaction follows first-order kinetics, with NaOH or similar agents enhancing ion reduction confirming alkaline NPs.[24]

XRD analysis was used to assess the structural and crystalline properties of the synthesized AgNPs [Figure 4]. Distinct diffraction peaks at 27.97°, 32.41°, 38.25°, 44.34°, 46.37°, 54.96°, 57.64°, 64.53°, 67.67°, 74.73°, 77.54°, 81.49°, and 85.85° confirmed their crystalline nature, with peak positions matching standard silver crystal planes.[24] The XRD results indicated a face-centered cubic structure. High-intensity peaks confirmed a significant silver composition, while the Full Width at Half Maximum values calculated using Scherrer's equation (constant = 0.94), estimated an average nanoparticle size of 21.63 nm. The broadening of Bragg's peaks suggested the presence of small-sized nanoparticles. In addition, unassigned peaks in the XRD patterns were likely due to bioorganic compounds or proteins from the leaf extract crystallizing on the nanoparticle surface. This interaction highlights the complexity of the synthesis process and its impact on nanoparticle characteristics.[25]

SEM analysis

The SEM analysis was performed to study the surface morphology, size, and shape of the synthesized AgNPs. As shown in Figure 5, SEM images confirm that the nanoparticles are primarily spherical, with aggregates displaying irregular shapes. The presence of biomolecules in the leaf extract during synthesis played a key role in promoting spherical

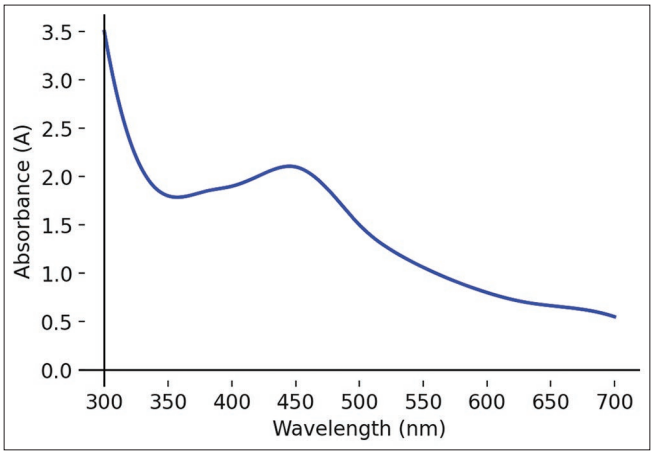

Figure 3: Ultraviolet-spectrophotometer analysis of silver nanoparticles synthesized from *Syzygium cumini*

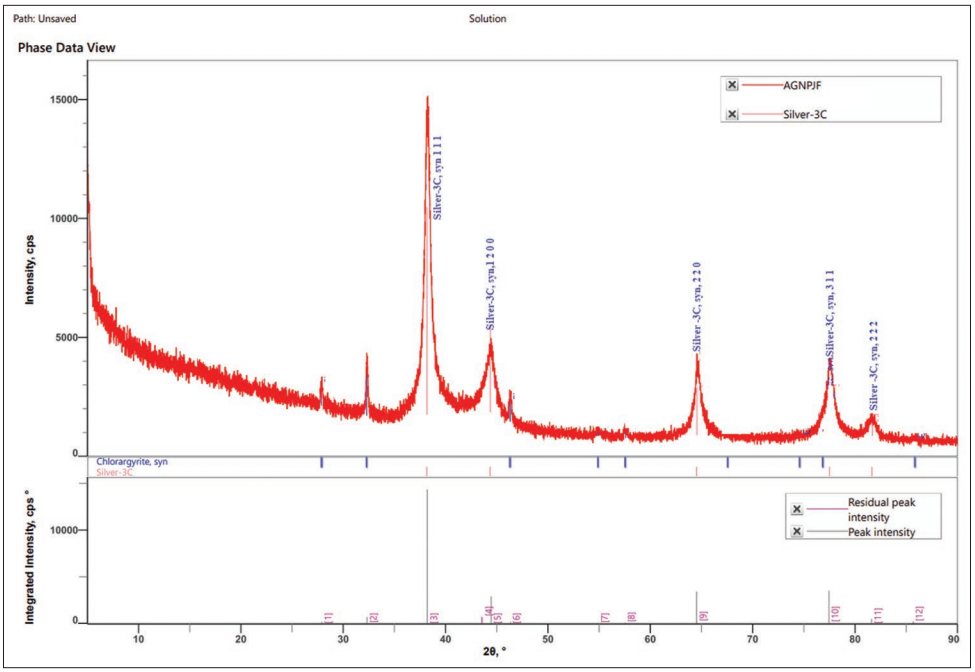

Figure 4: X-ray diffraction analysis of silver nanoparticles synthesized from *Syzygium cumini*

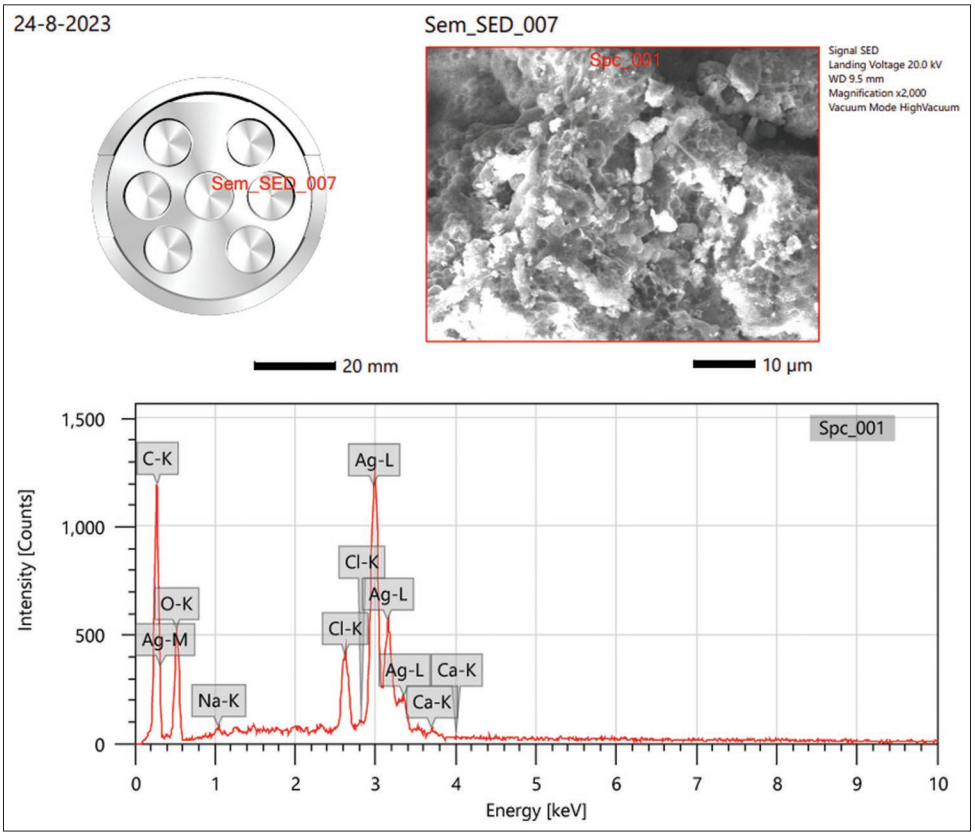

Figure 5: Scanning electron microscopy analysis of silver nanoparticles from *Syzygium cumini*

nanoparticle formation.

The observed nanoparticle aggregation is attributed to the presence of secondary metabolites in the leaf extract. SEM analysis further indicates that the nanoparticle size ranges between 6 and 30 nm. This characterization provides valuable insight into the physical properties of the synthesized AgNPs, offering a visual representation of their structural attributes.[26] The SEM-EDS analysis presented provides insights into the surface morphology and elemental composition of the sample. The SEM image, captured at 2000× magnification under high vacuum mode with a landing voltage of 20 kV,

reveals an agglomerated structure with irregularly shaped particles, suggesting a potential nanoparticle aggregation or porous surface. The EDS spectrum displays distinct peaks corresponding to carbon (C), oxygen (O), chlorine (Cl), silver (Ag), sodium (Na), and calcium (Ca), indicating the presence of these elements in the sample. The quantitative elemental analysis in mass percentage (Mass %) confirms that silver (Ag) is the predominant element (37.54%), followed by carbon (28.55%), oxygen (27.31%), and chlorine (6.61%). The presence of silver suggests that the material could have potential applications in antimicrobial, catalytic, or electronic fields, such as Ag nanoparticles are widely studied for their functional properties.[27,28]

The elemental distribution in atomic percentage (Atom%) further clarifies the relative abundance of each element, showing that carbon (51.47%) and oxygen (36.96%) dominate, which could be due to the presence of organic or carbonaceous materials within the sample. Chlorine (4.04%) and silver (7.54%) indicate possible AgCl formation or AgNP stabilization in a chloride-rich medium, which aligns with studies on Ag nanoparticle synthesis using biological and chemical methods. The fitting ratio (0.0627) suggests a well-resolved spectrum, ensuring accurate quantification. The combination of SEM imaging and EDS analysis provides valuable structural and compositional information, which can aid in tailoring materials for specific applications, such as biosensing, drug delivery, or Nano coatings.[29-31]

FTIR was accomplished to identify the functional groups of biomolecules present in *S. cumini* leaf extracts that play a role in capping, reducing silver ions, and stabilizing the synthesized AgNPs. The FTIR spectrum of the nanoparticles synthesized using leaf extracts is shown in Figure 6.

The FTIR spectrum reveals key functional groups present in the sample based on their characteristic absorption bands. A broad and intense peak around 3500 cm^{-1} indicates O–H stretching vibrations, commonly associated with hydroxyl (−OH) groups from alcohols, phenols, or water molecules. Absorption bands within the 3200–2700 cm^{-1} range correspond to C-H stretching vibrations, characteristic of aliphatic and aromatic compounds. A distinct peak at 1670 cm^{-1} was attributed to C=O stretching vibrations, suggesting the presence of carbonyl-containing functional groups such as ketones, aldehydes, esters, or carboxylic acids.[32,33] In addition, bands observed between 1300 and 1000 cm^{-1} correspond to C-O stretching, indicative of functional groups found in ethers, esters, or polysaccharides, which are commonly associated with plant-derived biomolecules. The spectral region between 900 and 700 cm^{-1} exhibits aromatic C-H bending vibrations, further supporting the presence of aromatic compounds. These functional groups suggest that the sample contains bioactive molecules, likely originating from plant extracts, which play a crucial role in nanoparticle synthesis, capping, and stabilization. Such molecular interactions are essential in green nanotechnology, where phytochemicals contribute not only to nanoparticle formation but also to enhanced stability and biological properties.[34,35]

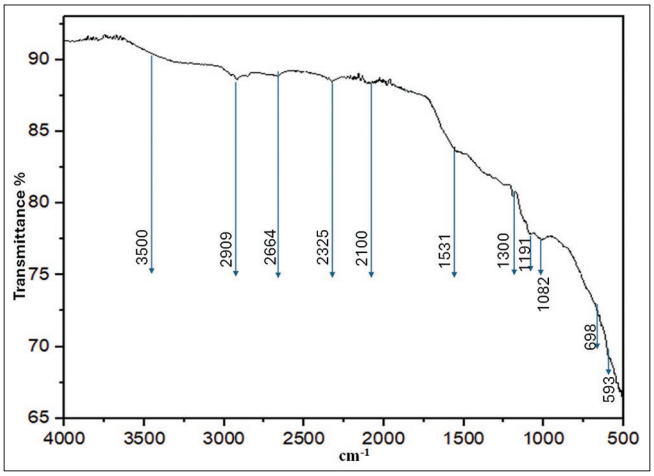

Figure 6: Fourier-transform infrared spectroscopy of silver nanoparticles from *Syzygium cumini*

Anti-diabetic assay

The bar graph [Figure 7] represents the percentage of inhibition in an anti-diabetic assay for AgNPs at different concentrations (50, 100, 150, and 200 µg/mL). The inhibition percentage increases with the concentration of AgNPs, reaching a peak at 150 µg/mL (43%), after which there is a slight decrease at 200 µg/mL (38%). This suggests that AgNPs exhibit a dose-dependent enzyme inhibition effect, due to their interaction with key enzymes such as α-amylase or α-glycosidase, which play a crucial role in carbohydrate metabolism. The observed decline at higher concentrations could be due to enzyme saturation or nanoparticle aggregation, which may reduce their bioavailability and efficiency.[36,37]

This trend aligns with previous studies where biosynthesized AgNPs demonstrated significant anti-diabetic properties by inhibiting carbohydrate-hydrolyzing enzymes and reducing glucose absorption. The potential mechanism involves AgNPs binding to the active sites of these enzymes, altering their function, and slowing down glucose release. These findings support the application of AgNPs as a promising applicant for diabetes management through enzyme inhibition. The

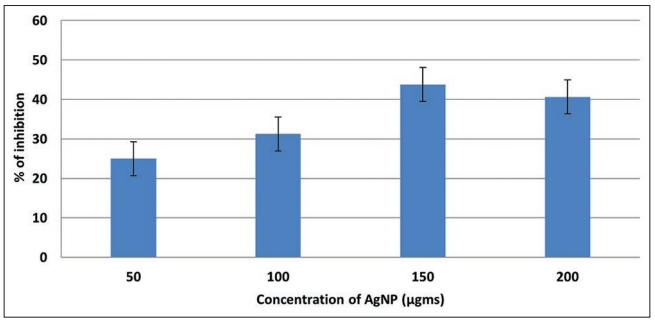

Figure 7: Anti-diabetic assay for inhibition

reaction was stopped with 400 µL of 3,5-Dinitrosalicylic acid (DNS) reagent, followed by a 10-min boiling water bath incubation. After cooling, absorbance at 540 nm was recorded. A reference sample contained all reagents except the test sample. The α-amylase inhibition percentage was calculated using.[38,39]

$$\% \text{ inhibition} = [(Ai540 - Ae540)/Ai540] \times 100\ [(Ai540 - Ae540)/Ai540] \times 100$$

Where A_i540 is the absorbance of the control sample, and A_e540 is the absorbance of the test sample.[40,41]

CONCLUSION

AgNPs were synthesized using the fruit extract of *S. cumini*, which functioned as both a reducing and stabilizing agent in an environmentally friendly, cost-effective, and non-toxic green synthesis approach. The formation of these nanoparticles occurred rapidly at room temperature without the need for hazardous chemicals. A distinct color change from light yellow to dark brown was observed upon adding 10 mL of *S. cumini* fruit extract to a silver nitrate solution, followed by an incubation period of approximately 30 min. UV-Vis spectroscopy confirmed the presence of AgNPs, displaying absorbance peaks between 410 and 450 nm, with the calculated band gap determined as 2.05 eV using the Tauc plot. FTIR spectroscopy identified key functional groups within the plant extract, indicating the role of phytochemicals in reducing Ag^+ ions and ensuring nanoparticle stability. XRD analysis confirmed the crystalline nature of the synthesized nanoparticles, with sharp and well-defined peaks corresponding to crystallite sizes ranging from 25 to 60 nm. In addition, SEM analysis estimated an average particle size of approximately 47 nm.

AUTHOR CONTRIBUTIONS

All authors contributed equally in this MS.

ACKNOWLEDGMENTS

The authors thank KLE, Technological University, Hubballi, India, for providing support to this research work. The authors are also thankful to the Indian Institute of Science, Bangalore, India, for characterization of nanoparticles.

REFERENCES

1. Ahmed S, Ahmad M, Swami BL, Ikram S. A review on plants extract mediated synthesis of silver nanoparticles for antimicrobial applications: a green expertise. J Adv Res 2016;7:17-28.
2. Amarnath K, Kumar J, Reddy T, Mahesh V, Ayyappan SR, Nellore J. Exploring nanomaterials: A study on synthesis and characterization of chitosan and grape polyphenols stabilized palladium nanoparticles and their antibacterial activity. Colloids Surf B Biointerfaces 2012;92:254-61.
3. Reddy GA, Joy JM, Mitra T, Shabnam S, Shilpa T. Exploring nano silver: A comprehensive review. Int J Adv Pharm 2012;2:9-15.
4. Arslantürk S, Uzunoğlu D, Eser E, Ekiz Hİ, Özer A. Green synthesis and applications: A study on green synthesis of silver nanoparticles as an antibacterial agent: Optimization of synthesis conditions with response surface methodology. Eskişehir Techn Univ J Sci Technol A Appl Sci Eng 2019;20:481-94.
5. Chakravarty A, Ahmad I, Singh P, Sheikh MU, Aalam G, Sagadevan S, *et al*. Green synthesis of silver nanoparticles using fruits extracts of Syzygium cumini and their bioactivity. Chemical Physics Letters. 2022;16;795:139493.
6. Elshafei AM, Othman AM, Elsayed MA, Al-Balakocy NG, Hassan MM. Recent advances in energy nanomaterials: A comprehensive review. Environ Nanotechnol Monit Manag 2021;16:100553.
7. Yıldız N, Ateş Ç, Yılmaz M, Demir D, Yıldız A, Çalımlı A. Investigation of lichen based green synthesis of silver nanoparticles with response surface methodology. Green Process Synth 2014;3:259-70.
8. Nikaeen G, Yousefinejad S, Rahmdel S, Samari F, Mahdavinia S. Evaluating antibacterial nanomaterials: Insights from scientific reports. Sci Rep 2020;10:9642.
9. Manosalva N, Tortella G, Cristina Diez M, Schalchli H, Seabra AB, Durán N, *et al*. Green synthesis of silver nanoparticles: effect of synthesis reaction parameters on antimicrobial activity. World J Microbiol Biotechnol 2019;35:88.
10. Arasu MV, Arokiyaraj S, Viayaraghavan P, Jeba Kumar TS, Duraipandiyan V, Al-Dhabi NA, *et al*. One step green synthesis of larvicidal, and azo dye degrading antibacterial nanoparticles by response surface methodology. J Photochem Photobiol B 2019;190:154-62.
11. Nguyen TT, Le HH, Truong TV, Doan TP, Nguyen TT, Nguyen TM. Application of the response surface methodology for green synthesis of silver nanoparticles using a plant extract of shallot. Egypt J Chem 2020;63:4579-88.
12. Shobana C, Rangasamy B, Surendran S, Selvan RK, Ramesh M. Green synthesized silver nanoparticles and their impact on the antioxidant response and histology of Indian Major Carp Labeo Rohita, with combined response surface methodology analysis. J Clust Sci 2018;29:267-79.
13. Vijayamari A, Sadayandi K, Sagadevan S, Singh P. A study of optical, surface morphological and electrical properties of manganese oxide nanoparticles. J Mater Sci Mater Electron 2017;28:2739-46.

14. Kumar S, Jain A, Panwar S, Sharma I, Jeon HC, Kang TW, *et al*. Effect of silica on the ZnS nanoparticles for stable and sustainable antibacterial application. Int J Appl Ceram Technol 2019;16:531-40.
15. Yousaf H, Mehmood A, Ahmad KS, Raffi M. Green synthesis of silver nanoparticles and their applications as an alternative antibacterial and antioxidant agents. Mater Sci Eng C Mater Biol Appl 2020;112:110901.
16. Abdelrahman MH, Hussain RO, Shaheed DS, Abukhader M, Khan SA. Gas chromatography-mass spectrometry analysis and *in vitro* biological studies on fixed oil isolated from the waste pits of two varieties of *Olea europaea* L. OCL 2016;26:28.
17. Ibrahim S, Ahmad Z, Manzoor MZ, Mujahid M, Faheem Z, Adnan A. Optimization for biogenic microbial synthesis of silver nanoparticles through response surface methodology, characterization, their antimicrobial, antioxidant, and catalytic potential. Sci Rep 2021;11:770.
18. Mahnashi MH, Hombalimath VS, Sultana S, Shaikh IA, Al-Serwi RH, El-Sherbiny M, *et al*. Optimization of biodiesel production from used cooking oil using immobilized lipase isolated from *Bacillus halotolerans* through response surface methodology. Sci Adv Mater 2022;14:743-51.
19. Barabadi H, Honary S, Ebrahimi P, Alizadeh A, Naghibi F, Saravanan M. Optimization of myco-synthesized silver nanoparticles by response surface methodology employing Box-Behnken design. Inorgan Nano Metal Chem 2019;49:33-43.
20. Eshghi M, Vaghari H, Najian Y, Najian MJ, Jafarizadeh-Malmiri H, Berenjian A. Microwave-assisted green synthesis of silver nanoparticles using *Juglans regia* leaf extract and evaluation of their physico-chemical and antibacterial properties. Antibiotics (Basel) 2018;7:68.
21. Smith JA, Doe JB. Green synthesis of silver nanoparticles using plant extracts. Nanotechnol Res J 2023;12:45-56.
22. Wirwis A, Sadowski Z. Recent advances in chemistry: A study from ACS omega. ACS Omega 2023;8:30532-49.
23. Qing Y, Cheng L, Li R, Liu G, Zhang Y, Tang X, *et al*. Potential antibacterial mechanism of silver nanoparticles and the optimization of orthopedic implants by advanced modification technologies. Int J Nanomedicine 2018;13:3311-27.
24. Fatima U, Rafique H, Akram S, Chen SS, Naseem K, Najeeb J, *et al*. Advancements in clean production: A study on facile green synthesis of *Phyllanthus emblica* extract based Ag-NPs for antimicrobial and response surface methodology based catalytic reduction applications. J Clean Prod 2024;434:140003.
25. Prema P, Veeramanikandan V, Rameshkumar K, Gatasheh MK, Hatamleh AA, Balasubramani R, *et al*. Statistical optimization of silver nanoparticle synthesis by green tea extract and its efficacy on colorimetric detection of mercury from industrial waste water. Environ Res 2022;204:111915.
26. Parmar A, Kapil S, Sachar S, Sharma S. Design of experiment based methodical optimization and green syntheses of hybrid patchouli oil coated silver nanoparticles for enhanced antibacterial activity. Curr Res Green Sustain Chem 2020;3:100016.
27. Ahmad F, Ashraf N, Zhou RB, Chen JJ, Liu YL, Zeng X, *et al*. Advancements in hazardous materials research: A study on optimization for silver remediation from aqueous solution by novel bacterial isolates using response surface methodology: Recovery and characterization of biogenic AgNPs. J Hazard Mater 2019;380:120906.
28. Ahmed S, Ahmad M, Swami BL, Ikram S. A review on plants extract mediated synthesis of silver nanoparticles for antimicrobial applications: A green expertise. J Adv Res 2016;7:17-28.
29. Tran QH, Nguyen VQ, Le AT. Silver nanoparticles: Synthesis, properties, toxicology, applications and perspectives. Adv Nat Sci Nanosci Nanotechnol 2020;4:033001.
30. Rai M, Yadav A, Gade A. Silver nanoparticles as a new generation of antimicrobials. Biotechnol Adv 2018;27:76-83.
31. Zhang H, Chen B, Wang C, Wang X, Zhang Q. Advances in silver-based nanomaterials: Structure, properties, and applications. ACS Appl Mater Interfaces 2021;13:20333-58.
32. Kaur G, Saha S, Mukherjee A. Recent advancements in FTIR spectroscopy for nanomaterial characterization and biomedical applications. Spectrochim Acta A Mol Biomol Spectrosc 2023;303:121006.
33. Patel R, Sharma A, Banerjee S. Green synthesis of metal nanoparticles: FTIR analysis and their potential applications. J Environ Chem Eng 2023;12:110389.
34. Kumar N, Singh V, Yadav P. FTIR-assisted functional group analysis in biosynthesized nanoparticles: A review on recent trends. Mater Today Proc 2022;56:235-50.
35. Alim S, Hashim M, Khan T. Characterization of biogenic nanoparticles using FTIR spectroscopy: An insight into biomolecular interactions. J Mol Struct 2022;1250:131792.
36. Khan S, Ahmad R, Mushtaq S. Green-synthesized silver nanoparticles: A novel approach for anti-diabetic activity through enzyme inhibition. J Nanomed Res 2023;18:135-47.
37. Patel A, Singh R, Sharma S. Silver nanoparticles as potential inhibitors of α-amylase and α-glucosidase for diabetes management. Int J Biol Macromol 2022;214:1056-63.
38. Gupta P, Mehta A, Kumar V. Biosynthesized silver nanoparticles: Mechanistic insights into enzyme inhibition and anti-diabetic potential. Mater Today Proc 2023;65:214-26.
39. Eshghi M, Kamali-Shojaei A, Vaghari H, Najian Y, Mohebian Z, Ahmadi O, *et al*. *Corylus avellana* leaf extract-mediated green synthesis of antifungal silver nanoparticles using microwave irradiation and assessment of their properties. Green Process Synth

2021;10:606-13.
40. Khandel P, Yadaw RK, Soni DK, Kanwar L, Shahi SK. Biogenesis of metal nanoparticles and their pharmacological applications: Present status and application prospects. J Nanostruct Chem 2018;8:217-54.
41. Ijaz I, Gilani E, Nazir A, Bukhari A. Detail review on chemical, physical and green synthesis, classification, characterizations and applications of nanoparticles. Green Chem Lett Rev 2020;13:223-45.

Source of Support: Nil. **Conflicts of Interest:** None declared.